

On Long-Wave Disturbances of Dynamic Height in the North Pacific¹

GUNNAR I. RODEN

Department of Oceanography, University of Washington Seattle 98195

(Manuscript received 26 May 1976, in revised form 24 August 1976)

ABSTRACT

Long-wave disturbances of dynamic height in the North Pacific are investigated by means of closely spaced STD (salinity, temperature, depth) stations and are related to atmospheric forcing. Wavelike disturbances with length scales between 400 and 600 km are common in the latitude range between 20° and 50°N. The wave amplitudes are larger in the western than in the central and eastern Pacific, and they depend upon season. A large eastward decrease in wave amplitude is observed near the Emperor seamount chain. The wavelike disturbances extend to several hundred meters' depth, with an exponential-type decrease in wave amplitude. The baroclinic currents associated with the dynamic height perturbations are an order of magnitude larger than the mean currents. The perturbations are related to atmospheric forcing, in particular the curl of the wind stress field. Where the distribution of the curl is zonal, meridional waves are excited, which are reflected in north-south dynamic height sections. Where several forcing regions by the curl of the wind stress coexist, the observed dynamic height sections show complex and asymmetric perturbations. The observed 400-600 km wavelengths are commensurate with planetary waves of diverse origin; the exact processes of their formation are poorly understood at present.

1. Introduction

The spatial distribution of dynamic height is of considerable interest to oceanographers because it determines the configuration of the baroclinic flow field, an important aspect in ocean dynamics. For any given time, the baroclinic flow field can be visualized as consisting of a mean flow field and a perturbation. The mean dynamic topography of the Pacific Ocean, based on conventional hydrographic casts with Nansen bottles, has been depicted by Reid (1961) and Wyrтки (1974) and is reasonably well known. The dominant features are the subtropical highs and the subpolar and equatorial lows, the position and extent of which vary with season and depth (Reid and Arthur, 1975). Typical length scales of these features are several thousand kilometers.

When closely spaced hydrographic stations are analyzed in detail, it is found that perturbations are superimposed upon the mean topography. These perturbations may be either wavelike, with typical length scales of hundreds of kilometers, or of an irregular kind consisting, for example, of a single steep slope, followed by minor undulations. In the central North Pacific, wavelike disturbances in the temperature field were first described by Bernstein and White (1974), who found scales between 300 and 500 km to be dominant. Dynamic height, however, is not only a function of tem-

perature, but also of salinity, and it is of interest to find out whether the spatial structure evident in the temperature field is reflected also in the geopotential field.

The origin of the wave-like disturbances with length scales of several hundred kilometers is attributed to planetary waves. In an ocean driven by traveling atmospheric disturbances and by differential heating and salt input, these waves are likely to be forced, rather than free. Moreover, the planetary waves interact with the complicated topography of the ocean bottom, creating in some cases standing and reflected wave patterns. It is no wonder, then, that difficulties arise when one tries to relate the observed wave patterns to simple mathematical models. Nevertheless, it is noteworthy that the observed wavelength can be explained by 1) traveling atmospheric disturbances (Longuet-Higgins, 1965; Lighthill, 1967); 2) stationary atmospheric disturbances of annual and semiannual frequency (Lighthill, 1967); Duing, 1970; Ivanov and Novitsky, 1975); 3) standing Rossby waves, in which the westward phase speed is balanced by a uniform eastward setting current of only a few centimeters per second (Pedlosky, 1971); and 4) reflection of Rossby waves from boundaries such as the Aleutians (Kinder *et al.*, 1975). The relative importance of the above mentioned processes cannot be assessed at the present time, but can be expected to vary from one geographic region to another.

In the following, a description is given of the spatial distribution of dynamic height in the North Pacific.

¹ Contribution No. 0928 from the Department of Oceanography, University of Washington, Seattle.

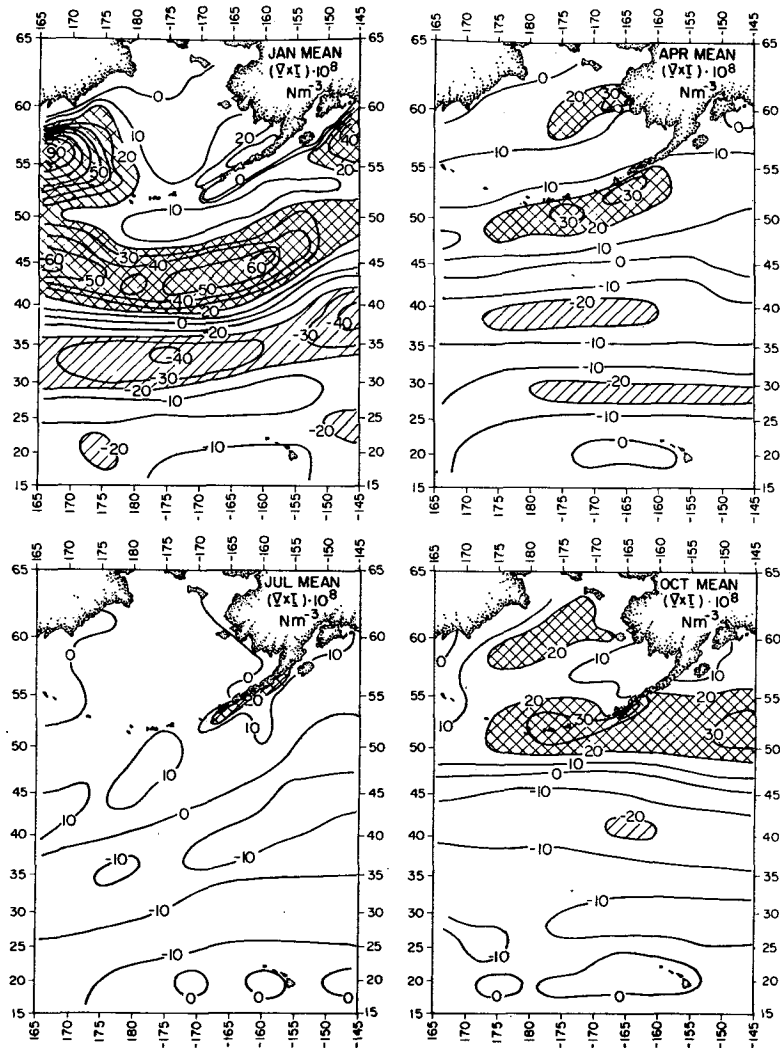


FIG. 1. Seasonal variation of the curl of the wind stress, based on a 1° latitude-longitude grid. Areas of strong positive curl are cross hatched; areas of strong negative curl are shaded by diagonal lines.

Emphasis is placed on wave-like perturbations observed in long sections of closely spaced stations, and some of the possible causes are discussed. Of these, atmospheric forcing is of particular importance, because a nonuniform wind stress field is known to generate planetary waves (Longuet-Higgins, 1965).

2. Data

The dynamic heights relative to 1500 db were computed from field measurements of temperature and salinity made on cruises of the R/V *Thomas G. Thompson* of the University of Washington during the years 1968–1975. On these cruises, stations were spaced 27–36 km apart on sections up to 2700 km long. The vertical sampling was at 3 m intervals between 0 and 1500 m and was done with a Plessey model 9006 STD and a model 9040 CTD, calibrated in the field. The integration of the specific volume anomaly was carried

out by utilizing all the data between 0 and 1500 m. The dynamic heights are expressed in units of J kg^{-1} , equivalent to 0.1 dynamic meter. An estimate of the geometric sea level height can be obtained by dividing the dynamic height values by the acceleration of gravity.

3. Spatial and temporal variations of the curl of the wind stress

The curl of the wind stress is an important driving force for planetary waves (Longuet-Higgins, 1965; Lighthill, 1967; 1969). In order to understand better the wave-like perturbations in dynamic height, it is necessary to take a brief look at the configuration of the curl field.

The mean seasonal variation of the vertical component of the curl of the wind stress for the central North Pacific is shown in Fig. 1. The figure is based on

the stress of the geostrophic wind, resolved on a 1° latitude-longitude grid. The close resolution is necessary to bring out the oceanographically relevant spatial features. It is seen that the distribution of the curl of the wind stress is predominantly zonal. Bands of negative curl occur to the south of the westwind maximum and to the north of the tradewind maximum and are related to subtropical and subarctic oceanic fronts (Roden, 1975). Bands of positive curl are found to the north of the westward maximum and are indicative of large-scale oceanic upwelling. The intensity of the wind stress curl and the position of the zonal bands varies with season. In the latitude belt between 40° and 45°N, the curl decreases from $6 \times 10^{-7} \text{ N m}^{-3}$ in winter to $-1 \times 10^{-7} \text{ N m}^{-3}$ in summer, indicating a seasonal change in sign. In subtropical latitudes the sign of the curl does not change, but the intensity decreases from $-4 \times 10^{-7} \text{ N m}^{-3}$ in January to $-1 \times 10^{-7} \text{ N m}^{-3}$ in July. The zonal distribution of the curl of the wind stress on long-term mean monthly time scales is also found when observed winds are used (Wyrtki and Meyers, 1975).

The predominantly zonal orientation of the wind stress curl in mid-ocean acts as a line source for planetary waves with mainly meridional wavenumbers, which can be detected in north-south dynamic height sections. It is important to consider not only the shape and intensity of forcing by the curl of the wind stress, but also the duration of forcing. If forcing is of an impulsive type, waves of all frequencies, however high, will be created; if the duration is finite, waves of low and moderately high, rather than very high frequency will be excited (Lighthill, 1969).

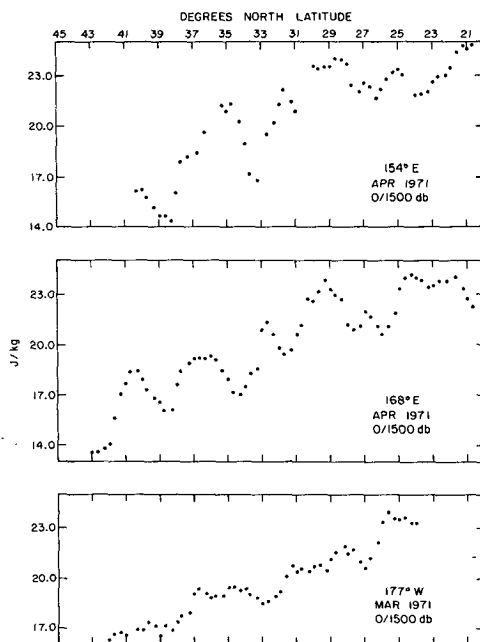


FIG. 2. Meridional profiles of dynamic height, relative to 1500 db, in the tropical western Pacific in April 1971.

4. Observed profiles of dynamic height

a. Western North Pacific

Meridional profiles of dynamic height along longitudes 154°E, 168°E and 177°W are shown in Fig. 2. The sections were occupied toward the end of the winter season when atmospheric forcing was strong. In all sections, wave-like disturbances with length scales between 400 and 500 km stand out. There is little variation of the wave pattern with latitude or longitude; on the other hand, waveheights vary considerably from one geographical region to another. The most pronounced change in waveheight takes place between longitudes 168°E and 177°W, with the heights in the western section being two to three times larger than in the eastern one. This agrees with investigations on the standard deviation of dynamic height in which it was found that the amplitudes in the western Pacific were about twice those in the central Pacific (Wyrtki, 1975).

The large change in waveheights between longitudes 168°E and 177°W cannot be attributed to the wind field alone, because atmospheric forcing at both longitudes was approximately the same (Roden, 1972). A possible explanation for the marked decrease in waveheight is the Emperor seamount chain, a major topographic feature, which extends in a NNW-SSE direction at approximately longitude 170°E. This submarine mountain range rises 3 to 4 km from the surrounding seafloor and comes to within 1 km of the sea surface in places; it is not an unbroken barrier, however, but has several large and deep gaps. The Emperor seamount chain has a decided effect upon the Kuroshio: usually well-defined by a high-speed core to the west (Kawai, 1972); it is hardly recognizable to the east (Roden, 1970, 1972). Apparently, the seamount chain acts as a perforated barrier, which is efficient in diffusing the energy of a strong current. Whether it is also efficient in diffusing the energy of planetary waves impinging upon it, is not known at present and needs to be investigated.

The presence of large amplitude planetary perturbations in the dynamic height profiles shown in Fig. 2 makes it difficult to define the North Pacific current and to determine its transport. To be meaningful, the North Pacific current should be defined in terms of the mean slope obtained by suitable filtering of long records. The mean slopes of dynamic height suggest eastward flow between latitudes 27° and 43°N. The speeds of the baroclinic flow associated with the mean slopes are quite low and vary between 0.04 and 0.08 m s^{-1} (Table 1). The speeds associated with the perturbations, on the other hand, are typically an order of magnitude larger, reach up to 0.6 m s^{-1} , and can be either to the eastward or westward.

b. Central North Pacific

Meridional profiles of dynamic height at longitude 158°W are shown in Fig. 3 as a function of pressure.

TABLE 1. Baroclinic flow, relative to 1500 db, associated with mean and perturbation slopes of dynamic height. All units are in m s^{-1} ; eastward and northward directions are positive.

Section	Mean speed	Perturbation speed (max)
North Pacific current between 27° and 41°N		
154°E, Apr 1971	0.08	0.58
168°E, Apr 1971	0.06	0.48
177°W, Mar 1971	0.04	0.23
158°W, Jan 1974	0.03	0.49
158°W, Apr 1968	0.03	0.10
158°W, Oct 1975	0.03	0.31
Tradewind current between 12° and 25°N		
143°W, Oct 1972	-0.05	0.41
133°W, Oct 1972	-0.04	0.25
California current between 117° and 153°W		
32°-33°N, Oct 1972	-0.01	-0.17

The prominent features are the perturbations with length scales between 400 and 600 m. The perturbations are in phase and of the same wavelength down to about the 600 db level. The wave amplitudes decrease exponentially with increasing pressure (depth): at latitude 32°N, this decrease is from 1 J kg^{-1} at 0 db, to 0.5 J kg^{-1} at 300 db, to 0.25 J kg^{-1} at 600 db, yielding a decay coefficient of 0.0023 per decibar (meter). The above implies that the size of the baroclinic perturbations in

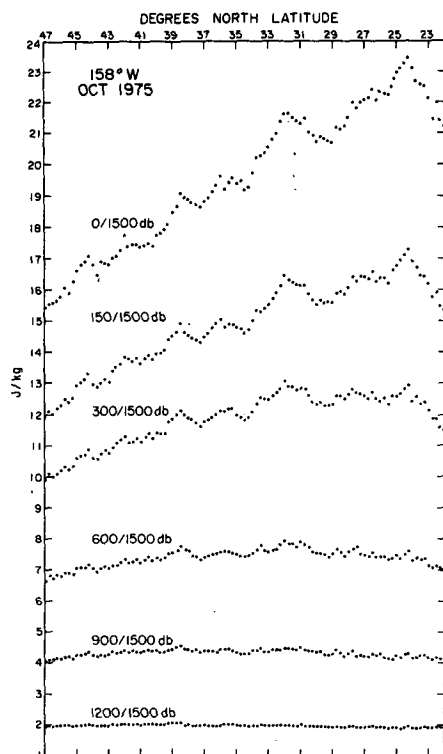


FIG. 3. Vertical variation of meridional dynamic height profiles relative to 1500 db in the central Pacific in October 1975.

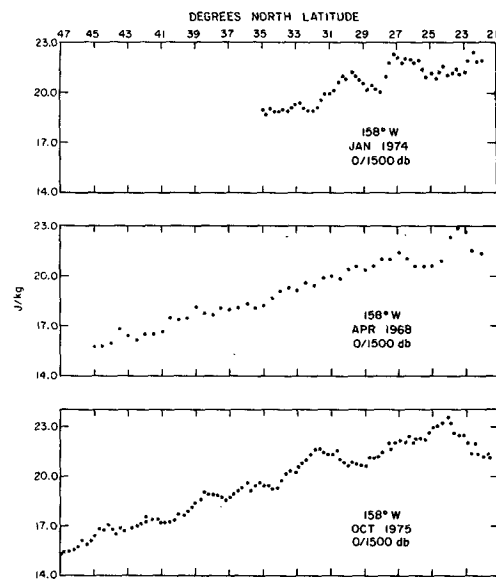


FIG. 4. Seasonal variation of meridional dynamic height profiles relative to 1500 db in the central Pacific.

the upper few hundred meters of the ocean is about the same and that the speed of flow associated with them decreases rather slowly with increasing depth.

The seasonal variation of dynamic profiles at longitude 158°W is indicated in Fig. 4. The *mean* slopes are quite small and show little seasonal variation, yielding a mean eastward current of 0.03 m s^{-1} in the latitude range between 27° and 47°N. The perturbation slopes, however, vary considerably with season and yield currents several times as strong (Table 1). The absence of seasonally variable mean flow and the dominance of time variable perturbation flow suggest that the mesoscale waves are related to atmospheric forcing.

In January 1974, the zone between 21° and 33°N was dominated by strong and steady easterly winds and perturbations with wavelengths of 300-500 km and amplitudes of about 1 J kg^{-1} were found. In April 1968, weak winds prevailed between latitudes 23° and 43°N and the perturbation amplitudes were small. In early October 1975, a few transient disturbances of moderate strength occurred north of 37°N; calms prevailed between 32° and 34°N, and well-developed trade winds were encountered south of 30°N. The primary atmospheric forcing region was in the trade wind belt, which explains the southward increase in perturbation amplitude.

The above findings are in agreement with studies of the spatial distribution of the standard deviation of dynamic height. For the mid-Pacific, Wyrтки (1975) finds a twofold southward increase in the standard deviation between latitudes 45° and 25°N and a decided lack of seasonal variation of the mean dynamic topography.

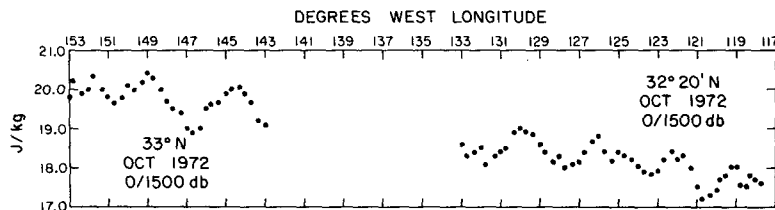


FIG. 5. Zonal profile of dynamic height relative to 1500 db in the subtropical eastern Pacific in October 1972.

c. Eastern North Pacific

The longitudinal distribution of dynamic height in the eastern subtropical Pacific is shown in Fig. 5. The section extends about 3300 km due west of the California-Mexico boundary and was occupied during the fall season when northerly winds were prominent. A meridionally oriented source of strong wind stress curl was present between 125° and 135°W, giving rise to planetary waves with predominantly zonal wavenumbers. These waves are clearly reflected in the zonal dynamic height profile shown. The waves are quite regular, with wavelengths of about 400 km and waveheights of the order of 1 J kg⁻¹. Wavelength and waveheight are almost independent of longitude. The oscillations are superimposed upon a gentle and uniform eastward slope. The mean current between 117° and 153°E is to the southward at 0.01 m s⁻¹. Currents associated with the oscillations are typically 0.1 m s⁻¹ and may be either to the northward or southward.

Meridional sections of dynamic height at longitudes 133°, 143° and 153°W are shown in Fig. 6. The sections cover the trade wind and subtropical regions of the eastern Pacific and were occupied in the fall season. Several sources for atmospheric forcing of planetary waves were present: a zonal band of positive wind stress curl between 10° and 15°N, a zonal band of negative wind stress curl between 20° and 25°N and a meridional band of positive wind stress curl between 125° and 135°W, to the north of 30°N (Roden, 1974). Because of the existence of several forcing regions, complicated planetary wave patterns can be expected.

Several interesting features stand out in the meridional dynamic height profiles. At 153°W, wavelike perturbations with length scales between 400 and 500 km are prominent. The wave heights decrease northward as one proceeds from the trade wind region toward the subtropical belt of low winds. This is expected as the wave energy decreases with distance from the forcing region. At 133° and 143°W, the outstanding features are the asymmetry of the perturbations to the south of 25°N and the virtual absence of perturbations to the north of this latitude. The features are not easy to explain. The asymmetry with the steeper slopes toward the north could result from the Ekman-type mass convergence near the northern trade wind boundary. The virtual absence of perturbations to the north of the trade wind boundary could conceivably result

from planetary wave interference, because of the proximity of several atmospheric forcing regions.

The mean slopes between 9° and 23°N are to the southward and suggest a mean westward baroclinic flow of 0.05 m s⁻¹, which can be identified with the trade wind current. The asymmetry of the perturbations is such that stronger eastward than westward baroclinic flow is encountered, a feature also noted by Seckel (1968). Maximum perturbation flow speeds are of the order of 0.4 m s⁻¹ (Table 1).

5. Theoretical aspects of planetary waves of 400–600 km scale

The observations of dynamic height in the North Pacific suggest planetary oscillations with length scales between 400 and 600 km. It is of interest to investigate briefly the properties of such waves and to speculate on the reasons for their existence. An exact theoretical deduction taking into account the nonuniform atmospheric forcing, the variable bottom topography and the inhomogeneous mean current field is not possible at present. Instead, several idealized but instructive examples will be given and their relevance discussed.

a. Free Rossby waves, no mean current

The wavenumbers are assumed known from observations, and it is desired to find the corresponding fre-

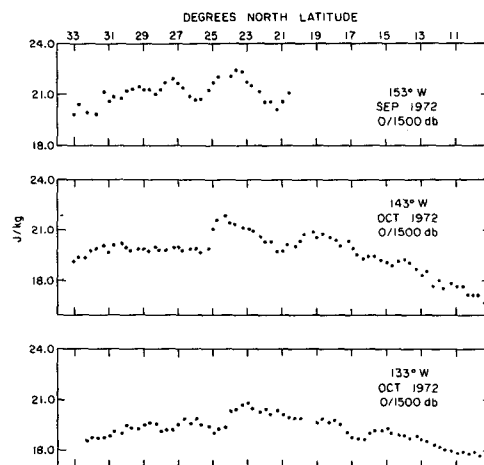


FIG. 6. Meridional profiles of dynamic height relative to 1500 db in the subtropical and trade wind regions of the eastern Pacific in October 1972.

TABLE 2. Frequencies (σ , s^{-1}), phase velocities (C_p , $m\ s^{-1}$) and group velocities (C_g , $m\ s^{-1}$) of free barotropic and baroclinic Rossby waves of 400 km length ($k, l = 1.57 \times 10^{-5}\ m^{-1}$) at different latitudes. Barotropic waves are for an ocean 4 km deep. Baroclinic waves are for a mixed layer depth of 100 m and a density ratio $\Delta(\rho/\rho) = 10^{-3}$.

Parameter	Latitude											
	1	4	15	30	45	60	1	4	15	30	45	60
	Barotropic						Baroclinic					
	Zonal waves ($l=0$)											
$\sigma \times 10^6$	1.45	1.45	1.40	1.24	1.02	0.73	1.41	1.01	0.20	0.05	0.02	0.01
$C_p \times 10^2$	9.23	9.23	8.94	7.93	6.51	4.61	8.97	6.47	1.30	0.35	0.14	0.07
direction	270	270	270	270	270	270	270	270	270	270	270	270
$C_g \times 10^2$	9.23	9.23	8.94	7.93	6.51	4.61	8.48	2.62	0.92	0.32	0.14	0.07
direction	090	090	090	090	090	090	090	090	270	270	270	270
	Meridional waves ($k=0$)											
σ	0	0	0	0	0	0	0	0	0	0	0	0
$C_p \times 10^2$	9.23	9.23	8.94	7.93	6.51	4.61	8.97	6.47	1.30	0.35	0.14	0.07
direction	270	270	270	270	270	270	270	270	270	270	270	270
	Oblique waves ($k=l$)											
$\sigma \times 10^6$	0.72	0.72	0.70	0.62	0.51	0.36	0.71	0.60	0.18	0.05	0.02	0.01
$C_p \times 10^2$	6.53	6.53	6.32	5.54	4.59	3.25	6.43	5.37	1.59	0.47	0.20	0.10
direction	225	225	225	225	225	225	225	225	225	225	225	225
$C_g \times 10^2$	4.61	4.61	4.47	3.97	3.25	2.30	4.49	3.19	0.09	0.31	0.14	0.07
direction	360	360	360	360	360	360	352	347	288	274	272	270

quencies, group velocities and phase velocities. This is easily obtained from the dispersion relation (Longuet-Higgins, 1965).

$$\sigma = -\beta k / (k^2 + l^2 + a^2); \quad a^2 = f^2 / gh, \quad (1)$$

where σ is frequency, k and l are the zonal and meridional wavenumbers, f is the Coriolis parameter, β its change with latitude, g is the acceleration of gravity and h is the ocean depth for barotropic waves, and $h = \Delta\rho h' / \rho$ for baroclinic waves, where $\Delta\rho$ is the density difference across the pycnocline and h' is the mixed layer depth.

The eastward and northward components of the group velocity are given by

$$\left. \begin{aligned} C_{gx} &= \beta(k^2 - l^2 - a^2) / (k^2 + l^2 + a^2)^2 \\ C_{gy} &= 2\beta kl / (k^2 + l^2 + a^2)^2 \end{aligned} \right\} \quad (2)$$

while those for the phase velocity are obtained from

$$\left. \begin{aligned} C_{px} &= -\beta / (k^2 + l^2 + a^2) \\ C_{py} &= -\beta k / l(k^2 + l^2 + a^2) \end{aligned} \right\} \quad (3)$$

Numerical examples for barotropic and baroclinic waves of 400 km wavelength are given in Table 2 as a function of latitude. The computations were done with $k, l = 1.57 \times 10^{-5}\ m^{-1}$, $h = 4\ km$, $h' = 100\ m$ and $\Delta\rho/\rho = 10^{-3}$. The term $a^2 = f^2/gh$ was found to be small compared to k and l for barotropic waves and large compared to k and l for nonequatorial baroclinic waves.

For zonal barotropic waves, ($l=0$) in deep ocean ($a \rightarrow 0$), the group and phase velocities are of equal magnitude but opposite direction. The phase velocity is to the west, and the group velocity is to the east with speeds between 0.04 and 0.09 $m\ s^{-1}$. For meridional

barotropic waves ($k=0$) the phase velocity vanishes, while the group velocity is to the west. For barotropic waves with $k=l$, the zonal component of the group velocity vanishes, while the meridional one is to the northward. The frequencies associated with the zonal barotropic waves vary between 10^{-6} and $1.5 \times 10^{-6}\ s^{-1}$ and correspond to periods between 2 and 3 months. Natural periods of this length are not prominent in the atmosphere (Roden, 1965), and hence, resonance of zonal waves with the atmosphere seems unlikely. On the other hand, baroclinic waves with large zonal wavenumbers have frequencies corresponding to the annual and semiannual periods of oscillation, and for such waves resonance with the atmosphere cannot be ruled out.

Baroclinic waves of 400 km length are strongly affected by the Coriolis term $a^2 = f^2/gh$, and the associated frequencies, group velocities, and phase velocities vary greatly with latitude. Poleward of 15° , the velocities are less than $0.01\ m\ s^{-1}$, and poleward of 45° , they are less than $0.001\ m\ s^{-1}$, which makes direct measurement difficult.

For zonal baroclinic waves, the direction of the group velocity changes sign where the wavelength equals the Rossby radius of deformation, here at about latitude 6° . Poleward of this latitude, the wave energy travels west; equatorward, east.² The significant feature is that in middle and high latitudes, the direction of the group

² For 400 km long waves, the maximum eastward velocity of $0.08\ m\ s^{-1}$ would occur at the equator, and the maximum westward velocity of slightly over $0.01\ m\ s^{-1}$ would occur at latitude 11° . Waves of 400 km length have yet to be found in equatorial latitudes, however.

velocity of baroclinic waves is *opposite* that of barotropic waves of the same wavelength. It would be most desirable to test this interesting theoretical result by direct measurements.

Meridional baroclinic waves, as in the barotropic case, have a zero phase velocity and a westward component of the group velocity. Baroclinic waves with $k=l$, unlike the barotropic case, have a nonvanishing westward component of the group velocity; for such waves the direction of wave energy propagation changes from northward at the equator to westward at latitudes 30–60°.

Frequencies associated with baroclinic waves of 400 km length vary between 10^{-8} and 10^{-6} s⁻¹, decreasing with increasing latitude. The frequency at latitude 15° equals the annual frequency. The trade winds, which dominate in this latitude, also show a strong annual signal. Resonance with the atmosphere is likely, therefore, in the trade wind region. Whether it occurs also in higher latitudes is not known at present because of the shortage of sufficiently long meteorological time series which would permit one to look for spectral peaks at very low frequencies.

b. Free Rossby waves, constant mean current

For a constant mean current V_0 making an angle α with the northern direction, the dispersion relation is given by

$$\sigma = V_0(k \sin\alpha + l \cos\alpha) - \beta k / (k^2 + l^2 + a^2). \quad (4)$$

The group and phase velocities can be obtained in the customary ways; they differ from expressions (2) and (3) only by additional terms involving the mean current. An interesting case occurs when the phase speed vanishes and the waves become standing Rossby waves. This happens when the mean current has the critical speed

$$V_{0c} = \frac{\beta k}{(k^2 + l^2 + a^2)(k \sin\alpha + l \cos\alpha)}, \quad (5)$$

which is equal to about 0.1 m s⁻¹ for barotropic waves of 400 km length and about 0.01 m s⁻¹ for baroclinic waves of the same length. Mean currents of this magnitude are quite common in the ocean and, hence, by implication, standing Rossby waves should be common also. The observed wave-like perturbations in the dynamic height profiles may be a reflection of this.

c. Forced Rossby waves, circular stationary storm

The case was investigated in detail by Longuet-Higgins (1965) assuming impulsive forcing in time. For a storm of quarter diameter r_0 , having a maximum windspeed W_{max} at a distance $2r_0$ from its center, the

wave amplitude is given by

$$\psi = \frac{3e^2\gamma\rho_a W_{max}t_0 r_0}{\rho_h\beta t} \left(\frac{(\kappa^2 + a^2)^{\frac{3}{2}}}{|(3k^2 - l^2)a^2 - \kappa^4|^{\frac{1}{2}}} \right) \times \left(\frac{4\kappa^2 r_0^2 - \kappa^4 r_0^4}{(1 + \kappa^2 r_0^2)^{7/2}} \right), \quad (6)$$

where $\kappa^2 = k^2 + l^2$, $e = 2.78 \dots$, ρ_a is the density of air, γ is the drag coefficient, and t is time. The wave amplitudes are strongly dependent upon the storm diameter $D = 4r_0$ and upon the "resonance factor" $(3k^2 - l^2)a^2 - \kappa^4$, which becomes zero at the latitude corresponding to $f^2 = gh\kappa^4 / (3k^2 - l^2)$. For barotropic waves in deep water, resonance is unlikely, because the term involving a^2 is small compared to κ^4 . For baroclinic waves resonance is unlikely at the equator, where a^2 vanishes, and in higher latitudes, where the a^2 term often exceeds the κ^4 term by an order of magnitude. For baroclinic waves of 400 km length of interest here, "resonance" is limited to a narrow band near latitude 4° and does not occur elsewhere. In latitudes poleward of about 6°, the wave amplitudes depend critically upon the size of the storm. The dependence is given by the last parentheses in (6). Maximum amplification occurs when the wavelength $L = 2.6D$; half of the maximum amplification occurs when $L = 1.5D$ and $L = 5D$; wave amplitudes become very small for $L \leq 0.75D$ and $L \geq 15D$. For 400 km waves to have been forced by a circular storm, the required storm diameters are in the range between 100 and 300 km, approximately. Such storms are rare in extratropical regions, where the observed storm diameters are typically of the order of 1000 km.

The above disagreement between theory and observation does not necessarily mean that circular extratropical storms cannot create waves of 400 km length. It only means that *impulse* type forcing in the time domain is not able to do so. To refine the theory, it is necessary to take into account the finite *duration* of the storm.

d. Forced Rossby waves, traveling transient disturbance

Planetary waves excited by traveling atmospheric disturbances of finite extent and duration were investigated by Lighthill (1967, 1969). If $0 \leq \sigma_0 \leq \rho_1$, where σ_0 is the frequency of forcing by the atmospheric disturbance and $\sigma_1 = 2/T_1$ is the highest frequency characteristic of the forcing effect (T_1 being the duration of the disturbance) and if the atmospheric disturbance progresses with constant speed V_0 making an angle α with the northward direction, the following characteristic equation is obtained:

$$[\sigma_0 + V_0(k \sin\alpha + l \cos\alpha)](k^2 + l^2 + a^2) = \beta k = 0. \quad (7)$$

The equation allows one to assess the character of barotropic and baroclinic Rossby waves in the wavenumber plane. The shape of the curves in the wavenumber

plane depends strongly upon the parameters $P_1 = \sigma_0 / (V_0 \beta)^{1/2}$ and $P_2 = (\beta g h / 4 f^2 V_0)^{1/2}$. If $a^2 = 0$ in (7), such as at the equator or, very nearly, when barotropic waves in deep water are considered, the relevant parameter is P_1 . For $P_1 < 1$ all waves of frequency $\sigma_0 < \sigma_1$ will be of a trailing character with small directional spread. For $P_1 \geq 1$ trailing as well as leading waves are generated, and the directional spread is large in the vicinity of the traveling disturbance. In the general case for $a^2 \neq 0$, waves will be of a trailing character with narrow directional spread when $P_1 > P_2$. To bring out the difference between barotropic and baroclinic cases, consider two typical examples. Firstly, assume a fast-moving storm of 4 days duration ($\sigma_1 = 1.82 \times 10^{-5} \text{ s}^{-1}$) moving ENE with a speed of 10 m s^{-1} near latitude 45°N . In the barotropic case $P_1 = 1.42$ for $\sigma_0 = \sigma_1$. Because all frequencies below the highest frequency σ_1 are important, the entire range $0 > P_1 \geq 1.42$ must be taken into account, meaning that the directional spread is large and that Rossby waves are found all around the disturbance. In the baroclinic case, with a mixed layer depth of 100 m and a density ratio $\Delta\rho/\rho = 10^{-3}$, one has $P_2 = 0.006$ and $P_1 \gg P_2$, which means that all Rossby waves trail the disturbance with narrow directional spread.

Secondly, consider a slow moving system with low frequency, such as the seasonal displacement of the subtropical high-pressure cells. Here, the duration is 6 months, so that $\sigma_1 = 3.98 \times 10^{-7} \text{ s}^{-1}$ and the speed of advance V_0 is of the order of 0.05 m s^{-1} . In this case, at latitude 30°N , $P_1 = 0.398$ and $P_2 = 0.136$ so that both in the barotropic and in the baroclinic states the planetary waves trail the disturbance with a narrow directional spread.

Finally, for disturbances stationary in space ($V_0 = 0$), but variable in time ($\sigma_0 \neq 0$), expression (7) reduces to

$$\sigma_0(k^2 + l^2 + a^2) + \beta k = 0, \quad (8)$$

which, in the wavenumber plane, is a circle of radius

$$R = (\beta^2 / 4\sigma_0^2), \quad (9)$$

which shrinks to a point when $\sigma_0 = (gh)^{1/2} / 2f$. For deep water ($h = 4 \text{ km}$) barotropic waves, this occurs when $\sigma_0 = 1.58 \times 10^{-5} \text{ s}^{-1}$ or $T = 4.4$ days; for baroclinic waves ($h = 100 \text{ m}$, $\Delta\rho/\rho = 10^{-3}$) this happens when $\sigma_0 = 7.77 \times 10^{-8} \text{ s}^{-1}$ or $T = 2.7$ years (both examples are for latitude 45°). A point in the wavenumber plane is equivalent to waves of constant length in the x - y plane. The physical interpretation is that when the frequency of oscillation of the atmospheric disturbance is near the cutoff frequency for Rossby waves, waves of constant length can be excited. For barotropic waves in mid-latitudes, this is measured in days; for baroclinic waves—in years. The time variations in the wind field are frequently peaked at a period of a few days, but convincing peaks with a period of a few years have yet to be found in mid-latitude wind spectra. Therefore,

Rossby waves of constant wavelength, if at all excited by a stationary atmospheric disturbance of time variable intensity, are likely to be of the barotropic kind.

6. Conclusions and suggestions for future research

The following conclusions can be drawn from an examination of closely spaced dynamic height sections and highly resolved wind stress fields:

- 1) Wavelike perturbations of dynamic height with length scales between 400 and 600 km are common in the North Pacific.
- 2) The perturbations are more pronounced in the western than in the central and eastern parts of the ocean. The largest decrease in wave amplitude takes place in the vicinity of the Emperor seamount chain, a major topographic feature.
- 3) The perturbations extend from the sea surface to a depth of several hundred meters. In the central Pacific, the wavelength is almost independent of depth and the wave amplitude decreases with depth slowly in an exponential fashion.
- 4) The baroclinic currents associated with dynamic height perturbations are often an order of magnitude stronger than the mean flow, complicating the definition of the North Pacific current.
- 5) There is some evidence that the perturbations are related to atmospheric forcing, particularly the curl of the wind stress field. In the central Pacific, the curl field is predominantly zonal and varies strongly with season. This excites predominantly meridional waves, the amplitude of which depends upon season. There is almost no seasonal variation of the mean baroclinic field in the mid-Pacific.
- 6) During late summer and early fall, the perturbation amplitudes decrease northward in the central Pacific. A plausible assumption is that the wave amplitudes decrease with distance from the forcing region. The main forcing during this time of the year is in the trade winds, and, as the waves propagate into the calmer regions to the north, the wave amplitudes decrease.
- 7) The observed dynamic height perturbations with 400–600 km length scales are commensurate with several theories of free and forced Rossby waves. The exact mechanisms of the formation of Rossby waves of this length scale are poorly understood at present, however. The difficulty arises from the fact that in nature the waves result from complicated interactions of nonuniform atmospheric forcing, variable bottom topography, and an inhomogeneous mean current field.

There are several outstanding questions to be solved in connection with perturbations of dynamic height. The link between atmospheric forcing and the wave-

like perturbations needs be investigated more fully and the response times established. Further evidence is needed for the decrease of perturbation amplitude with distance from the forcing region and of the dissipation mechanisms involved. The influence of large-scale topographic features upon planetary waves, such as the Emperor seamount chain and the Hawaiian ridge, deserves careful study.

The findings presented here are for the open North Pacific far from continental boundaries. Different perturbation patterns of dynamic height may occur in regions close to such boundaries. Theoretical studies (Longuet-Higgins, 1965; Lighthill, 1969; Pedlosky, 1971) have shown that, near such boundaries, incident and reflected planetary waves give rise to eddy-like flow patterns, which can propagate toward the interior of the ocean. Eddies in the dynamic height topography have been observed both in the western (Kawai, 1972) and the eastern Pacific coastal areas (Defant, 1950; Reid *et al.*, 1963), but a firm link between these observations and the planetary waves has yet to be established.

Acknowledgments. I am indebted to M. Rattray and L. H. Larsen for fruitful discussions. C. A. Barnes and R. H. Fleming offered advice. The scientific and operational crew of the R/V *Thomas G. Thompson*, Captains R. Schelling and Clampitt commanding, are to be commended for outstanding performance. The research reported herein was supported by the Office of Naval Research under Contract N-00014-75C-0502.

REFERENCES

- Bernstein, R. L., and W. B. White, 1974: Time and length scales of baroclinic eddies in the central North Pacific Ocean. *J. Phys. Oceanogr.*, **4**, 613-624.
- Defant, A., 1950: Reality and illusion in oceanographic surveys. *J. Mar. Res.*, **9**, 120-144.
- Duing, W., 1970: The monsoon regime of the currents of the Indian Ocean. *International Indian Ocean Expeditions Oceanographic Monographs*, Vol. 1, 1-68.
- Ivanov, Yu. A., and A. G. Novitsky, 1975: Reaction of the ocean to annual and semiannual atmospheric oscillations. *Okeanolog.*, **15**, 786-789.
- Kawai, H., 1972: Hydrography of the Kuroshio extension. *Kuroshio, Physical Aspects of the Japan Current*, H. Stommel and K. Yoshida, Eds., University of Washington Press, 235-352.
- Kinder, T. H., L. K. Coachman and J. A. Galt, 1975: The Bering slope current system. *J. Phys. Oceanogr.*, **5**, 231-244.
- Lighthill, M. J., 1967: On waves generated in dispersive systems by travelling forcing effects, with applications to the dynamics of rotating fluids. *J. Fluid. Mech.*, **27**, 725-752.
- , 1969: Unsteady wind driven ocean currents. *Quart. J. Roy. Meteor. Soc.*, **95**, 675-688.
- Longuet-Higgins, M. S., 1965: The response of a stratified ocean to stationary or moving wind systems. *Deep-Sea Res.*, **12**, 923-973.
- Pedlosky, J., 1971: Geophysical fluid dynamics. *Mathematical Problems in the Geophysical Sciences, Lectures in Applied Mathematics*, Vol. 13, Amer. Math. Soc., 1-60.
- Reid, J. L., 1961: On the geostrophic flow at the surface of the Pacific Ocean with respect to the 1000 decibar surface. *Tellus*, **13**, 489-502.
- , and R. S. Arthur, 1975: Interpretation of maps of geopotential anomaly for the deep Pacific Ocean. *J. Mar. Res.*, **33**, Suppl., 37-52.
- , R. A. Schwartzlose and D. M. Brown, 1963: Direct measurements of a small surface eddy off northern Baja, California. *J. Mar. Res.*, **21**, 205-218.
- Roden, G. I., 1965: On atmospheric pressure oscillations along the Pacific coast of North America. *J. Atmos. Sci.*, **22**, 280-295.
- , 1970: Aspects of the mid-Pacific transition zone. *J. Geophys. Res.*, **75**, 1097-1109.
- , 1972: Temperature and salinity fronts at the boundaries of the subarctic and subtropical transition zone in the western Pacific. *J. Geophys. Res.*, **77**, 7155-7187.
- , 1974: Thermohaline structure, fronts, and sea-air energy exchange of the trade wind region of Hawaii. *J. Phys. Oceanogr.*, **4**, 168-182.
- , 1975: On North Pacific temperature, salinity, sound velocity and density fronts and their relation to the wind and energy flux fields. *J. Phys. Oceanogr.*, **5**, 557-571.
- Seckel, G. R., 1968: A time sequence oceanographic investigation in the North Pacific tradewind zone. *Trans. Amer. Geophys. Union*, **49**, 377-387.
- Wyrtki, K., 1974: The dynamic topography of the Pacific ocean and its fluctuations, Hawaii Institute of Geophys. Rep. HIG-74-5, 19 pp., 37 figs. (contains bimonthly maps of dynamic height and standard deviations).
- , 1975: Fluctuations of the dynamic topography in the Pacific Ocean. *J. Phys. Oceanogr.*, **5**, 450-459.
- , and G. Meyers, 1975: The tradewind field over the Pacific Ocean. Hawaii Institute of Geophysics Rep. HIH-75-1, 26 pp., 25 figs. (contains mean monthly maps of observed winds and bimonthly maps of the divergence of the wind and the curl of the wind stress).